

# NMR Spectroscopic Investigations of Mixed Aggregates Underlying Highly Enantioselective 1,2-Additions of Lithium Cyclopropylacetylide to Quinazolines

Rodney L. Parsons, Jr.,<sup>\*,†</sup> Joseph M. Fortunak,<sup>†</sup> Roberta L. Dorow,<sup>†</sup> Gregory D. Harris,<sup>†</sup> Goss S. Kauffman,<sup>†</sup> William A. Nugent,<sup>†</sup> Mark D. Winemiller,<sup>‡</sup> Timothy F. Briggs,<sup>‡</sup> Bosong Xiang,<sup>‡</sup> and David B. Collum<sup>\*,‡</sup>

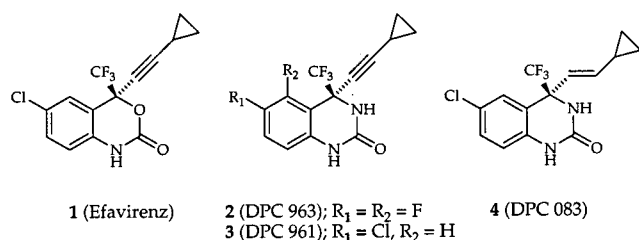
Contribution from DuPont Pharmaceuticals, Chemical Process Research and Development, Chambersworks, PRF-112, Deepwater, New Jersey 08023, and Department of Chemistry and Chemical Biology, Baker Laboratory, Cornell University, Ithaca, New York 14853-1301

Received March 1, 2001

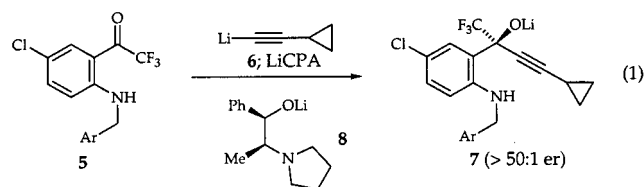
**Abstract:** The solution structures of mixed aggregates derived from lithium alkoxides and lithium acetylides were investigated as part of a program to develop practical syntheses of quinazolinone-based nonnucleoside reverse transcriptase inhibitors. Low-temperature <sup>6</sup>Li, <sup>13</sup>C, and <sup>15</sup>N NMR spectroscopies reveal that mixtures of lithium cyclopropylacetylide (RCCLi), a (+)-carene-derived amino alkoxide (R\*OLi), and lithium hexamethyldisilazide (LiHMDS) in THF/pentane afford a (RCCLi)<sub>3</sub>(R\*OLi) mixed tetramer, a C<sub>2</sub>-symmetric and asymmetric (RCCLi)<sub>2</sub>(R\*OLi)<sub>2</sub> mixed tetramer, and a C<sub>3</sub>-symmetric (RCCLi)(R\*OLi)<sub>3</sub> mixed tetramer. Analogous mixtures of RCCLi/R\*OLi in Et<sub>2</sub>O and Me<sub>2</sub>NEt also provide 3:1, 2:2, and 1:3 mixed tetramers. The stereochemistry of aggregation is highly sensitive to the medium. The C<sub>2</sub>-symmetric (RCCLi)<sub>2</sub>(R\*OLi)<sub>2</sub> mixed tetramer is formed in Et<sub>2</sub>O, whereas the asymmetric isomer is formed in Me<sub>2</sub>NEt. LiHMDS in THF is shown to be an efficient proton scavenger without forming LiHMDS–RCCLi or LiHMDS–R\*OLi mixed aggregates. LiHMDS–RCCLi mixtures form mixed aggregates in Me<sub>2</sub>NEt.

## Introduction

Several new classes of potent nonnucleoside reverse transcriptase inhibitors have been developed by DuPont Pharmaceuticals and Merck Research Laboratories.<sup>1</sup> Efavirenz (**1**) is now widely prescribed under the names Sustiva and Stocrin for the treatment of AIDS and symptomatic HIV-1 infection.<sup>2–4</sup> Although Efavirenz requires only once-daily dosing, is well tolerated, and exhibits outstanding viral suppression even for protease-sparing treatment regimens,<sup>2</sup> second-generation drug candidates **2**, **3**, and **4** possess significant activity against wild-type HIV and mutant strains resistant to currently approved drug regimens.<sup>1,5,6</sup> Compounds **2**, **3**, and **4** have entered advanced clinical trials.<sup>5</sup>



Over 50 000 kg of Efavirenz have been prepared by a highly enantioselective 1,2-addition of lithium cyclopropylacetylide (LiCPA, **6**) to trifluoromethyl ketone **5** (eq 1).<sup>3,4,7–9</sup> As part of



syntheses of **4** and its analogues, the DuPont group began investigating enantioselective additions of LiCPA to quinazolin-

(2) Young, S. D.; Britcher, S. F.; Tran, L. O.; Payne, L. S.; Lumma, W. C.; Lyle, T. A.; Huff, J. R.; Anderson, P. S.; Olsen, D. B.; Carroll, S. S.; Pettibone, D. J.; O'Brien, J. A.; Ball, R. G.; Balani, S. K.; Lin, J. H.; Chen, I.-W.; Schleif, W. A.; Sardana, V. V.; Long, W. J.; Byrnes, V. W.; Emini, E. A. *Antimicrob. Agents Chemother.* **1995**, *39*, 2602.

(3) Pierce, M. E.; Parsons, R. L., Jr.; Radesca, L. A.; Lo, Y. S.; Silverman, S.; Moore, J. R.; Islam, Q.; Choudhury, A.; Fortunak, J. M.; Nguyen, D.; Luo, C.; Morgan, S. J.; Davis, W. P.; Confalone, P. N.; Chen, C. Y.; Tillyer, R. D.; Frey, L.; Tan, L. S.; Xu, F.; Zhao, D. L.; Thompson, A. S.; Corley, E. G.; Grabowski, E. J. J.; Reamer, R.; Reider, P. J. *J. Org. Chem.* **1998**, *63*, 8536. Thompson, A. S.; Corley, E. G.; Huntington, M. F.; Grabowski, E. J. *J. Tetrahedron Lett.* **1995**, *36*, 8937.

(4) Efavirenz is currently being prepared by an amino alcohol-mediated addition of alkynyl zinc derivatives. Tan, L.; Chen, C. Y.; Tillyer, R. D.; Grabowski, E. J. J.; Reider, P. J. *Angew. Chem., Int. Ed. Engl.* **1999**, *38*, 711. Chen, C. Y.; Tan, L. S. *Enantiomer* **1999**, *4*, 599.

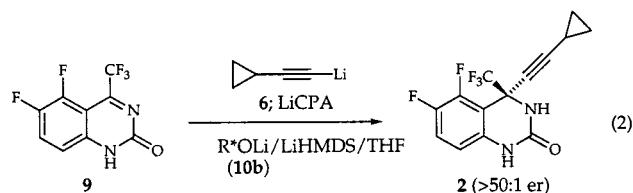
(5) Tucker, T. J.; Lyle, T. A.; Wiscount, C. M.; Britcher, S. F.; Young, S. D.; Sanders, W. M.; Lumma, W. C.; Goldman, M. E.; O'Brien, J. A.; Ball, R. G.; Homnick, C. F.; Schleif, W. A.; Emini, E. A.; Huff, J. R.; Anderson, P. S. *J. Med. Chem.* **1994**, *37*, 2437. Corbett, J. W.; Ko, S. S.; Rodgers, J. D.; Bachelier, L. T.; Klabe, R. M.; Diamond, S.; Lai, C. M.; Rabel, S. R.; Saye, J. A.; Adams, S. P.; Trainor, G. L.; Anderson, P. S.; Erickson-Viitanen, S. K. *Antimicrob. Agents Chemother.* **1999**, *43*, 2893. Corbett, J. W.; Ko, S. S.; Rodgers, J. D.; Gearhart, L. A.; Magnus, N. A.; Bachelier, L. T.; Diamond, S.; Jeffrey, S.; Klabe, R. M.; Cordova, B. C.; Garber, S.; Logue, K.; Trainor, G. L.; Anderson, P. S.; Erickson-Viitanen, S. K. *Antimicrob. Agents Chemother.* **1999**, *43*, 2893.

<sup>†</sup> DuPont Pharmaceuticals.

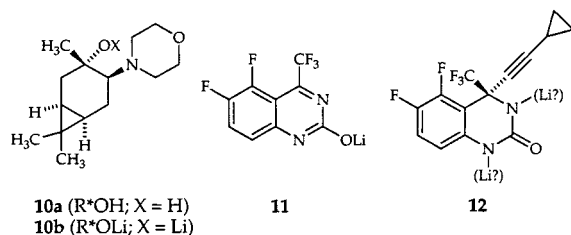
<sup>‡</sup> Cornell University.

(1) For a review of the syntheses of nonnucleoside reverse transcriptase inhibitors, see: Parsons, R. L., Jr. *Curr. Opin. Drug Discov. Dev.* **2000**, *3*, 783.

ones bearing an unprotected N–H group (eq 2). It is not



surprising that the mixtures of LiCPA and lithium ephedrate **8** used to prepare Efavirenz provided limited stereocontrol when applied to **9**.<sup>1</sup> Structural and mechanistic studies showed that the 1,2-addition to ketone **5** is based on a series of delicately balanced mixed aggregate equilibria.<sup>10,11</sup> Moreover, the N–H moiety of ketone **5** is not lithiated during the 1,2-addition,<sup>10</sup> whereas **9** is lithiated to afford **11** quantitatively under the reaction conditions, leaving considerable doubts about whether the 1,2-additions to ketone **5** and quinazolinone **9** are mechanistically analogous.



Using an iterative strategy in which synthetic organic methods and strategies for optimization were interwoven with organolithium structural and mechanistic studies, we developed a highly efficient and enantioselective synthesis of **2** and related derivatives as illustrated in eq 2.<sup>6</sup> We began with an extensive survey of conditions to find an effective combination of reagents, solvents, and temperatures (Chart 1).<sup>12</sup> (+)-3-Carene-derived amino alkoxide **10b** showed promising results and was subjected to further studies. Although amino alcohol **10a**<sup>13</sup> could be

(6) Kauffman, G. S.; Harris, G. D.; Dorow, R. L.; Stone, B. R. P.; Parsons, R. L., Jr.; Pesti, J. A.; Magnus, N. A.; Fortunak, J. M.; Confalone, P. N.; Nugent, W. A. *Org. Lett.* **2000**, *2*, 3119.

(7) For enantioselective addition of lithium acetylides to aldehydes mediated by amino alkoxides, see: Ye, M. C.; Logaraj, S.; Jackman, L. M.; Hillegass, K.; Hirsh, K. A.; Bollinger, A. M.; Grosz, A. L.; Mani, V. *Tetrahedron* **1994**, *50*, 6109. For other examples, see: Mukaiyama, T.; Soai, K.; Sato, T.; Shimizu, H.; Susuki, K. *J. Am. Chem. Soc.* **1979**, *101*, 1455. Schön, M.; Naef, R. *Tetrahedron: Asymmetry* **1999**, *10*, 169. Gärtner, P.; Letschnig, M.; Knollmüller, M. *Monatsh. Chem.* **2000**, *131*, 867. Knollmüller, M.; Ferencic, M.; Gärtner, P. *Tetrahedron: Asymmetry* **1999**, *10*, 3969. Gärtner, P.; Letschnig, M.; Knollmüller, M. *Monatsh. Chem.* **2000**, *131*, 867.

(8) For reviews of enantioselective 1,2-additions, see: Hurn, D. M. In *Comprehensive Organic Synthesis*; Trost, B. M., Fleming, I., Eds.; Pergamon: New York, 1991; Vol. 1, Chapter 1.2, p 49. Denmark, S. E.; Nicaise, O. J.-C. In *Comprehensive Asymmetric Catalysis*; Jacobsen, E. N., Pfaltz, A., Yamamoto, Y., Eds.; Springer-Verlag: Heidelberg, 1999; Chapter 26.2. Kobayashi, S.; Ishitani, H. *Chem. Rev.* **1999**, *99*, 1069. Steinig, A. G.; Spero, D. M. *Org. Prepr. Proc. Int.* **2000**, *32*, 205. Bloch, R. *Chem. Rev.* **1998**, *98*, 1407. Enders, D.; Reinhold, U. *Tetrahedron: Asymmetry* **1997**, *8*, 1895.

(9) Amino alkoxide/RLi mixtures have been investigated as superbases: Caubere, P. *Chem. Rev.* **1993**, *93*, 2317. Choppin, S.; Gros, P.; Fort, Y. *Org. Lett.* **2000**, *2*, 803.

(10) Thompson, A.; Corley, E. G.; Huntington, M. F.; Grabowski, E. J. J.; Remenar, J. F.; Collum, D. B. *J. Am. Chem. Soc.* **1998**, *120*, 2028.

(11) Xu, F.; Reamer, R. A.; Tillyer, R.; Cummins, J. M.; Grabowski, E. J. J.; Reider, P. J.; Huffman, J. C.; Collum, D. B. *J. Am. Chem. Soc.* **2000**, *122*, 11212.

(12) The selectivities depicted in Chart 1 are derived from protocols that include some variation, and, as a consequence, should be viewed only as representative.

recycled by extraction, minimizing excess LiCPA was a considerable economic concern.

A number of variables proved to be important determinants of selectivity and reaction efficiency.

(1) Aging: Optimum selectivities were obtained only if solutions of LiCPA and **10b** were aged at 60 °C before adding **9**. Previous investigations of the 1,2-addition in eq 1 showed that considerable “aging effects” stemmed from surprisingly slow organolithium aggregate exchange.

(2) Lithium bases: 1,2-Additions of LiCPA (**6**) tended to decelerate markedly at incomplete conversion. A survey of a number of lithium bases to serve as proton scavengers revealed that lithium hexamethyldisilazide (LiHMDS) improved the percent conversion, enantioselectivity, and reproducibility.

(3) Stoichiometry: Selectivities varied considerably with changes in the proportions of the LiCPA and **10b**, with optimum selectivities observed when 3.0 equiv of alkoxide **10b** are employed.

(4) Solvents: The best results were obtained using THF. The selectivities also improved when the reaction vessel was purged of the *n*-butane derived from *n*-BuLi.

(5) Substituents: The enantioselectivities depended somewhat on the relatively remote substituent on the lithium acetylide, and they fell off precipitously using simple alkylolithiums.

From an organolithium structural perspective, we must predicate our understanding of the enantioselectivity in eq 2 on a thorough understanding of the mixed aggregates derived from five lithium salts: LiCPA, **10b**, **11**, **12**, and LiHMDS. There are a total of 26 binary, ternary, quaternary, and quintary combinations. Each combination could provide a unique distribution of mixed aggregates that depends markedly on solvent, temperature, concentration, and stoichiometry.<sup>15</sup>

We describe herein NMR spectroscopic studies showing that lithium alkoxide **10b**, LiCPA, and LiHMDS yield mixed aggregates in proportions that are sensitive to the choice of coordinating solvent and hydrocarbon cosolvent. We will report the effects of lithium salts **11** and **12** on aggregate structures as well as investigations of structure–reactivity relationships in due course.

## Results

**NMR Spectroscopy: General Methods.** [<sup>6</sup>Li]LiCPA was prepared >98% <sup>6</sup>Li enriched and isolated as a white solid as described previously.<sup>10</sup> Although lithium caranolate **10b** could be isolated as a white solid, a more convenient and more reproducible protocol involves generating **10b** in situ from caranol **10a** using stock solutions of recrystallized [<sup>6</sup>Li]-LiHMDS.<sup>16</sup> A slight excess of LiHMDS ensures quantitative lithiation of the cyclopropylacetylene and alcohol **10a**. The <sup>6</sup>Li resonances of the LiHMDS dimer and monomer<sup>17</sup> confirm that adequate base was added.

Unusual solution aging effects on the enantioselectivities that we had previously attributed to slow mixed aggregate ex-

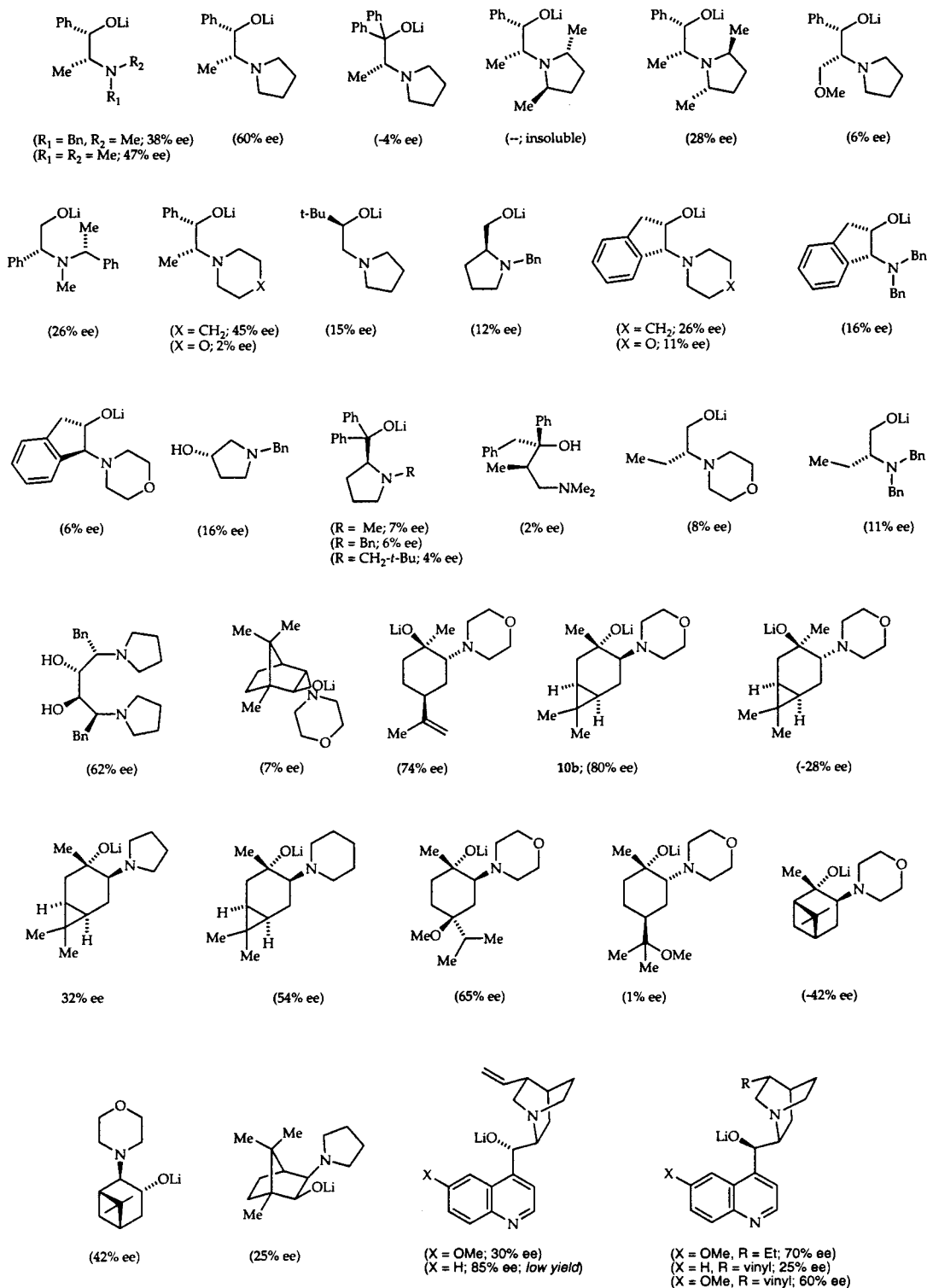
(13) Fedyunina, I. V.; Plemenkov, V. V.; Bikbulatova, S.; Nikitina, L. E.; Litvinov, I. A.; Kataeva, O. N. *Chem. Nat. Compd.* **1992**, *28*, 173.

(14) Although the *n*-butane derived from 10 M *n*-BuLi represents a significant increase in hydrocarbon concentration on large scale, certainly other changes affiliated with the purging process could be involved.

(15) For leading references to structural studies of RLi/R\*OLi mixed aggregates, see: Thomas, R. D.; Huang, H. *J. Am. Chem. Soc.* **1999**, *121*, 11239. Lochmann, L. *Eur. J. Inorg. Chem.* **2000**, 1115. Sorger, K.; Schleyer, P. v. R.; Stalke, D. *J. Am. Chem. Soc.* **1996**, *118*, 6924. Jackman, L. M.; Rakiewicz, E. F. *J. Am. Chem. Soc.* **1991**, *113*, 1202. Kremer, T.; Harder, S.; Junge, M.; Schleyer, P. v. R. *Organometallics* **1996**, *15*, 585.

(16) Romesberg, F. E.; Bernstein, M. P.; Gilchrist, J. H.; Harrison, A. T.; Fuller, D. J.; Collum, D. B. *J. Am. Chem. Soc.* **1993**, *115*, 3475.

(17) Lucht, B. L.; Collum, D. B. *J. Am. Chem. Soc.* **1995**, *117*, 9863.

**Chart 1.** Enantioselectivities for the Addition of LiCPA (3.0 equiv) to Quinazolinone **9** (eq 2) in the Presence of Ligands (2.5 equiv) Listed Below<sup>a</sup>

<sup>a</sup> Negative numbers refer to the opposite enantioselectivity

change<sup>10</sup> were also observed for mixtures of LiCPA and alkoxide **10b** (see below).<sup>18</sup> Accordingly, all samples were aged at room temperature for >10 min prior to low-temperature spectroscopic analyses unless noted otherwise.

<sup>6</sup>Li, <sup>13</sup>C, and <sup>15</sup>N NMR spectroscopic data are summarized in Table 1. Selected NMR spectra are shown in Figures 1–5. Additional spectra are included as Supporting Information. The complex spectra (exemplified by Figure 1G) were deconvoluted by several methods: (1) <sup>1</sup>J(<sup>6</sup>Li, <sup>13</sup>C)-resolved spectroscopy

deconvolutes the complex envelopes of <sup>6</sup>Li multiplets by providing the <sup>6</sup>Li–<sup>13</sup>C coupling along the orthogonal y-axis (Figure

(18) For other examples of slow aggregate exchanges and potentially related aging effects in organolithium chemistry, see: Lucht, B. L.; Collum, D. B. *J. Am. Chem. Soc.* **1994**, *116*, 7949. Basu, A.; Beak, P. *J. Am. Chem. Soc.* **1996**, *118*, 1575. Meyers, A. I.; Lutomshi, K. A.; Laucher, D. *Tetrahedron* **1988**, *44*, 3107. Baudouy, R.; Delbecq, F.; Gore, J. *J. Organomet. Chem.* **1979**, *177*, 39. Reich, H. J.; Holladay, J. E.; Mason, J. D.; Sikorski, W. H. *J. Am. Chem. Soc.* **1995**, *117*, 12137. Basu, A.; Gallagher, D. J.; Beak, P. *J. Org. Chem.* **1996**, *61*, 5718 and references therein.

**Table 1.**  $^6\text{Li}$ ,  $^{13}\text{C}$ , and  $^{15}\text{N}$  NMR Spectroscopic Data<sup>a</sup>

compd	solvent	$\delta$ $^6\text{Li}$ (m, $J_{\text{Li}-\text{C}}$ )	$\delta$ $^{13}\text{C}$ (m, $J_{\text{Li}-\text{C}}$ )	$\delta$ $^{15}\text{N}$ (m, $J_{\text{Li}-\text{N}}$ )
<b>6</b>	THF	0.047 (t, 9.2 Hz)	118.9 (qn, 9.2 Hz)	
		0.036 (qt, -)	113.8 (br, m)	
<b>15</b>	THF	1.1 (br)		
		0.0 (br)		
<b>16</b>	THF	1.16 (t, 6.6 Hz)	114.5 (m)	37.6 (t, 3.1 Hz)
		-0.11 (d, 4.2 Hz)		
<b>17</b>	THF	1.29 (dd, 6.2 Hz)	114.2 (m)	37.9 (t, 3.1 Hz)
		0.78 (d, 4.6 Hz)	114.4 (m)	38.0 (t, 2.7 Hz)
		0.02 (d, 4.5 Hz)		
<b>21</b>	THF	-0.16 (dd, 6.7, 4.2 Hz)		
		0.89 (d, 5.2 Hz)	116.6 (br, m)	38.7 (t, 2.7 Hz)
		-0.05 (s)		
<b>15</b>	toluene	1.33 (dd, 6.3 Hz)	114.7 (m)	38.2 (t, 3.1 Hz)
		0.20 (dd, 5.5 Hz)	115.2 (m)	
		0.10 (ddd, 3.2, 5.6, 6.6 Hz)	115.6 (m)	
		-0.05 (dd, 3.2, 5.6 Hz)		
<b>16</b>	toluene	1.21 (t, 6.5 Hz)	115.7 (m)	37.9 (t, 2.8 Hz)
		-0.18 (d, 4.0 Hz)		
<b>17</b>	toluene	1.37 (dd, 6.8, 4.5 Hz)	115.2 (m)	38.2 (t, 2.8 Hz)
		0.76 (d, 6.1 Hz)	116.6 (m)	38.3 (t, 2.8 Hz)
		0.01 (d, 4.5 Hz)		
<b>21</b>	toluene	-0.19 (dd, 6.8, 4.0 Hz)		
		0.80 (d, 5.8 Hz)	117.3 (br, m)	38.9 (t, 2.7 Hz)
		-0.18 (s)		
<b>13</b>	$\text{Me}_2\text{NEt}$	1.60 (d, 10.5 Hz)	112.5 (qn, 10.5 Hz)	43.6 (qn, 3.1 Hz)
<b>14</b>	$\text{Me}_2\text{NEt}$	2.00 (d, 5.9 Hz)	112.9 (br m)	45.6 (tt, 4.0, 3.4 Hz)
		1.29 (d, 7.2 Hz)		
		1.59 (dd, 6.1 Hz)	114.9 (m)	38.5 (t, 3.4 Hz)
<b>15</b>	$\text{Me}_2\text{NEt}$	0.64 (ddd, 6.0, 5.4, 3.0 Hz)	115.1 (m)	
		0.42 (dd, 5.3, 2.6 Hz)	115.4 (m)	
		0.28 (dd, 5.5 Hz)		
		1.85 (dd, 6.0, 2.0 Hz)	116.5 (m)	39.2 (t, 3.1 Hz)
<b>17</b>	$\text{Me}_2\text{NEt}$	1.21 (d, 5.2 Hz)	117.8 (m)	39.0 (t, 2.7 Hz)
		0.26 (dd, 5.4, 2.0 Hz)		
		0.20 (d, 5.0 Hz)		
<b>21</b>	$\text{Me}_2\text{NEt}$	1.28 (d, 5.5 Hz)	117.7 (m)	37.8 (t, 2.8 Hz)
		0.26 (s)		
		1.62 (dd)	113.8 (m)	38.3 (t, 2.7 Hz)
<b>15</b>	$\text{Et}_2\text{O}$	0.39 (ddd)	113.9 (m)	
		0.29 (dd)	114.4 (m)	
		-0.02 (dd)		
<b>16</b>	$\text{Et}_2\text{O}$	1.66 (t, 6.5 Hz)	114.9 (m)	38.2 (t, 3.1 Hz)
		0.07 (d, 4.0 Hz)		
<b>21</b>	$\text{Et}_2\text{O}$	1.28 (d, 5.5 Hz)	117.0 (m)	39.6 (t, 2.8 Hz)
		0.19 (s)		

<sup>a</sup> The  $J_{\text{C-Li}}$  coupling constants were routinely measured from the  $^1J(^6\text{Li}, ^{13}\text{C})$ -resolved spectrum. The multiplicities are denoted as follows: s = singlet, d = doublet, t = triplet, qt = quartet, qn = quintet, m = multiplet, br m = broad multiplet. The  $^6\text{Li}$ ,  $^{13}\text{C}$ , and  $^{15}\text{N}$  chemical shifts are reported relative to 0.3 M  $^6\text{LiCl}/\text{MeOH}$  at  $-90^\circ\text{C}$  ( $\delta$   $^6\text{Li}$  = 0.0 ppm), neat dimethylethylamine ( $\delta$   $^{15}\text{N}$  = 25.7 ppm), and the methyl group of neat toluene ( $\delta$   $^{13}\text{C}$  = 20.4 ppm), respectively. All  $J$  values are reported in hertz.

2).<sup>19</sup> (2)  $^6\text{Li}, ^{13}\text{C}$ -heteronuclear multiple quantum correlation (HMQC) spectroscopy<sup>20,21</sup> (Figure 3) and  $^6\text{Li}, ^{15}\text{N}$ -HMQC spectroscopy<sup>21,22</sup> (Figure 4) provide coupling data and the Li-C and Li-N connectivities. (3)  $^6\text{Li}, ^6\text{Li}$ -exchange spectroscopy ( $^6\text{Li}, ^6\text{Li}$ -EXSY)<sup>23</sup> reveals the fluxional properties of the chelates

(19) (a) Günther, H.; Moskau, D.; Bast, P.; Schmalz, D. *Angew. Chem., Int. Ed. Engl.* **1987**, *26*, 1212. (b) Braun, S.; Kalinowski, H. O.; Berger, S. *150 and More Basic NMR Experiments*, 2nd ed.; Wiley-VCH: New York, 1998; p 350.

(20) Günther, H. *J. Braz. Chem.* **1999**, *10*, 241. Mons, H.-E.; Günther, H.; Maercker, A. *Chem. Ber.* **1993**, *126*, 2747. Günther, H. In *Advanced Applications of NMR to Organometallic Chemistry*; Gielen, M., Willem, R., Wrackmeyer, B., Eds.; Wiley & Sons: Chichester, 1996; Chapter 9.

(21) Xiang, B.; Winemiller, M. D.; Briggs, T. F.; Fuller, D. J.; Collum, D. B. *J. Magn. Reson.* **2000**, in press.

(22) Gilchrist, J. H.; Harrison, A. T.; Fuller, D. J.; Collum, D. B. *Magn. Reson. Chem.* **1992**, *30*, 855. Review: Gudat, D. *Annu. Rep. NMR Spectrosc.* **1999**, *38*, 139.

(23) Orrell, K. G. *Annu. Rep. NMR Spectrosc.* **1999**, *37*, 1. Perrin, C. L.; Dwyer, T. J. *Chem. Rev.* **1990**, *90*, 935. Hilmersson, G.; Davidsson, Ö. *Organometallics* **1995**, *14*, 912 and references therein.

(Figure 5), providing intraaggregate relationships that complement the connectivities derived from scalar couplings.

**Homoaggregates.** LiCPA previously was shown to be a dimer-tetramer equilibrium in THF/pentane solution (Figure 1A, Table 1).<sup>10</sup> LiCPA is insoluble in  $\text{Et}_2\text{O}$  and forms a single prismatic oligomer in  $\text{Me}_2\text{NEt}$ .<sup>24,25</sup>

Solutions of  $[\text{Li}]\mathbf{10b}$  in THF/pentane or THF/toluene solutions show three major  $^6\text{Li}$  resonances (Figure 1B). Analogous  $^6\text{Li}$  spectra recorded on solutions of  $[\text{Li}, ^{15}\text{N}]\mathbf{10b}$  show a doublet for each resonance, indicating coordination by a morpholino group. Similarly,  $^6\text{Li}$  NMR spectra recorded on  $[\text{Li}, ^{15}\text{N}]\mathbf{10b}$  in  $\text{Et}_2\text{O}$  or  $\text{Me}_2\text{NEt}$  solutions show predominantly two  $^6\text{Li}$  resonances, each coupled to a morpholino group (Supporting Information.) Although the resonances may stem from various stereoisomeric prismatic oligomers,<sup>26</sup> the spec-

(24) For extensive references to structural studies of lithium acetylides, see ref 7.

(25) Breslin, S. R.; Winemiller, M. D.; Briggs, T. F.; Collum, D. B. Unpublished.

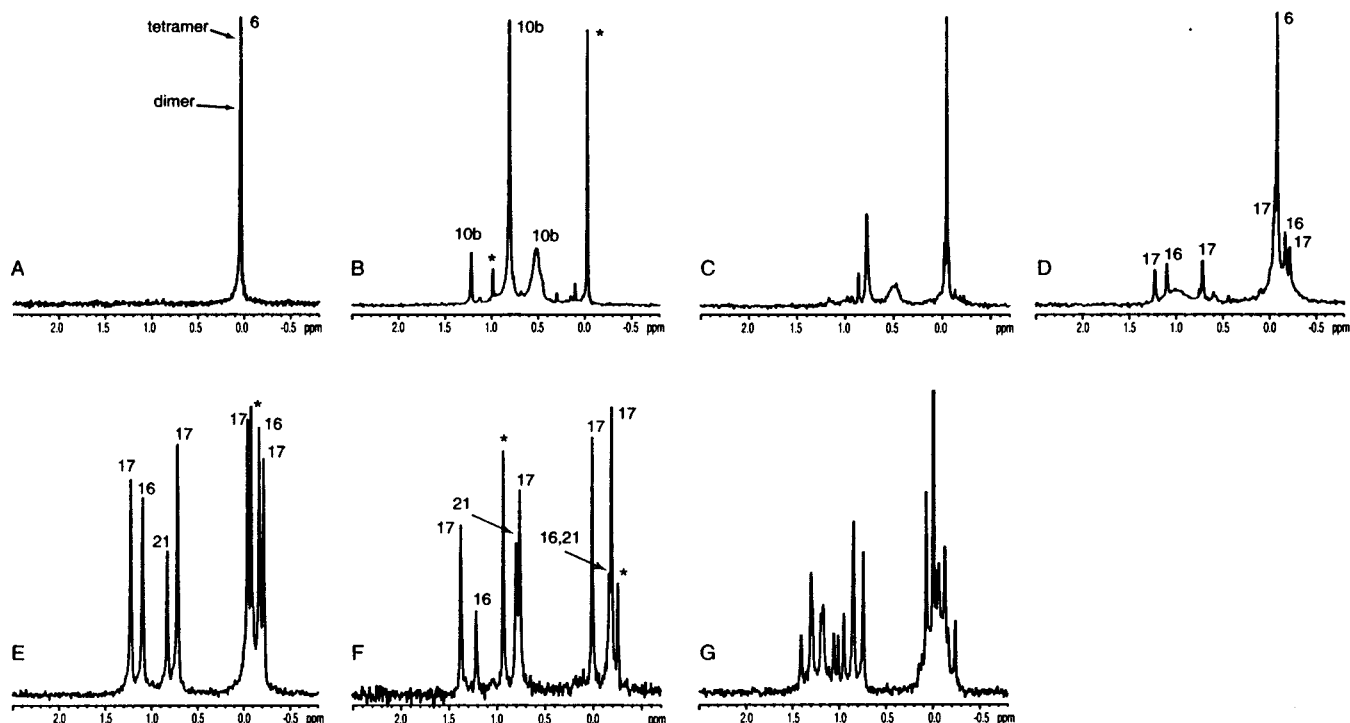


**Figure 1.**  $^6\text{Li}$  NMR spectra recorded at  $-115\text{ }^\circ\text{C}$  of 80% THF/pentane solutions containing residual  $[\text{LiHMDMS}]$  (marked by an asterisk, \*) and the following: (A)  $[\text{Li}]\text{LiCPA}$ ; (B)  $[\text{Li}]\text{10b}$ ; (C) a 1:1 mixture of  $[\text{Li}]\text{LiCPA}$  and  $[\text{Li}]\text{10b}$  prior to aging; (D) a 3:1 mixture of  $[\text{Li}]\text{LiCPA}$  and  $[\text{Li}]\text{10b}$  after aging; (E) a 1:1 mixture of  $[\text{Li}]\text{LiCPA}$  and  $[\text{Li}]\text{10b}$ ; (F) a 1:1 mixture of  $[\text{Li}]\text{LiCPA}$  and  $[\text{Li}]\text{10b}$  in 3:1:1 toluene/THF/pentane; and (G) a 1:1 mixture of  $[\text{Li},^{13}\text{C}]\text{LiCPA}/[\text{Li}]\text{10b}$ .

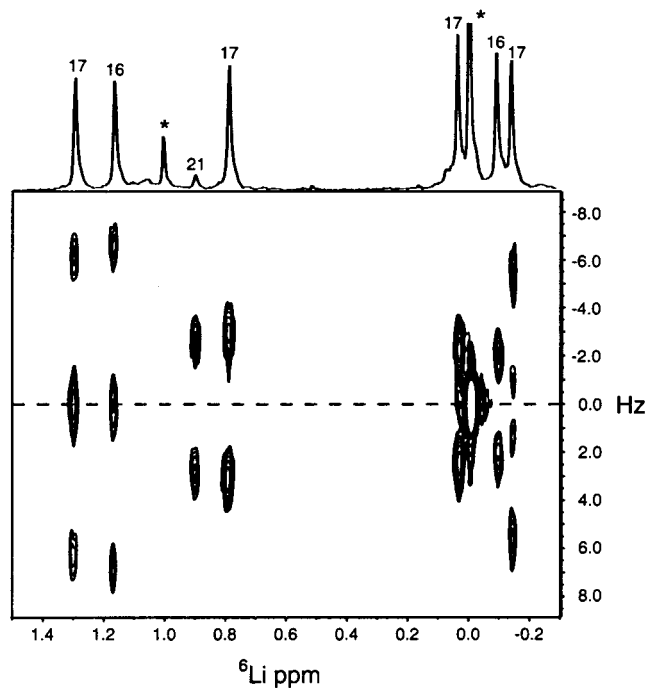


**Figure 2.**  $J$ -resolved spectrum of a 1:1 mixture of  $[\text{Li},^{13}\text{C}]\text{LiCPA}$  (0.2 M) and  $[\text{Li}]\text{10b}$  (0.2 M) in 80% THF/pentane at  $-115\text{ }^\circ\text{C}$  showing mixed tetramers **16**, **17**, and **21**. LiHMDMS is indicated by an asterisk (\*).

troscopically opaque Li–O linkages preclude structural assignments.

**LiHMDMS Mixed Aggregates.** Control experiments using  $[\text{Li},^{15}\text{N}]\text{LiHMDMS}$  confirmed<sup>16</sup> that LiHMDMS does not form mixed aggregates with LiCPA or **10b** in THF solutions.<sup>27</sup> In the poorly coordinating solvents  $\text{Et}_2\text{O}$  and  $\text{Me}_2\text{NEt}$ ,<sup>27,28</sup> however,

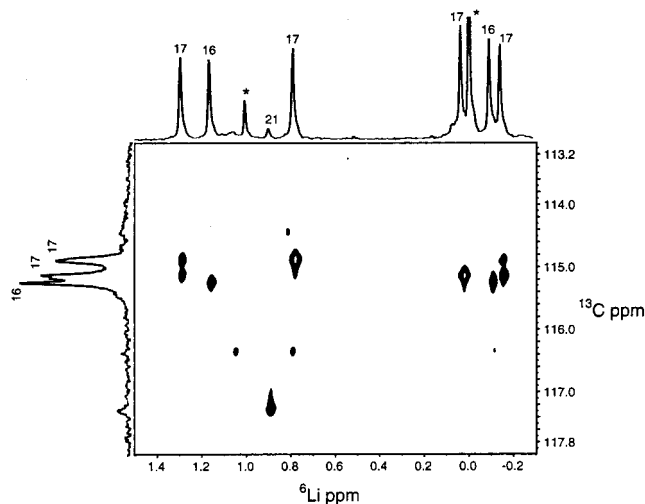


**Figure 3.**  $^6\text{Li},^{13}\text{C}$ -HMQC spectrum recorded on a 1:1 mixture of  $[\text{Li},^{13}\text{C}]\text{LiCPA}$  (0.2 M) and  $[\text{Li}]\text{10b}$  (0.2 M) in 80% THF/pentane at  $-115\text{ }^\circ\text{C}$  showing mixed tetramers **16**, **17**, and **21**. LiHMDMS is indicated by an asterisk (\*).

the behavior is more complex.<sup>29–31</sup>  $[\text{Li}]\text{LiHMDMS}/[\text{Li},^{13}\text{C}]\text{LiCPA}$  and  $[\text{Li},^{15}\text{N}]\text{LiHMDMS}/[\text{Li}]\text{LiCPA}$  mixtures in  $\text{Me}_2\text{NEt}$

(26) Setzer, W. N.; Schleyer, P. v. R. *Adv. Organomet. Chem.* **1985**, *24*, 353. Seebach, D. *Angew. Chem., Int. Ed. Engl.* **1988**, *27*, 1624.

(27) Lucht, B. L.; Collum, D. B. *Acc. Chem. Res.* **1999**, *32*, 1035.

(28) Brown, T. L.; Gerteis, R. L.; Rafus, D. A.; Ladd, J. A. *J. Am. Chem. Soc.* **1964**, *86*, 2135. Settle, F. A.; Haggerty, M.; Eastham, J. F. *J. Am. Chem. Soc.* **1964**, *86*, 2076. Lewis, H. L.; Brown, T. L. *J. Am. Chem. Soc.* **1970**, *92*, 4664. Quirk, R. P.; Kester, D. E. *J. Organomet. Chem.* **1977**, *127*, 111.

(29) Collum, D. B. *Acc. Chem. Res.* **1993**, *26*, 227.

(30) For mixed aggregates of general structure  $\text{R}_2\text{N}(\text{Li}/\text{R}'\text{OLi})$ , see: Sun, C. Z.; Williard, P. G. *J. Am. Chem. Soc.* **2000**, *122*, 7829 and references therein.

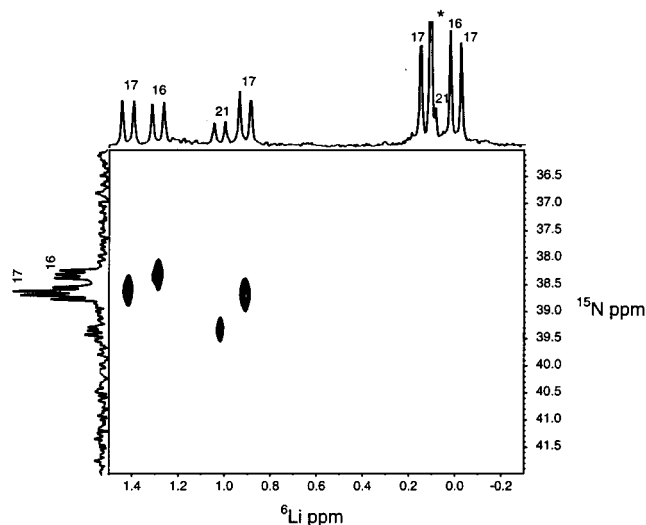


**Figure 4.**  $^6\text{Li},^{15}\text{N}$ -HMQC spectrum recorded on a 1:1 mixture of  $[\text{}^6\text{Li}]\text{LiCPA}$  (0.2 M) and  $[\text{}^6\text{Li},^{15}\text{N}]\mathbf{10b}$  (0.2 M) in 80% THF/pentane at  $-115\text{ }^\circ\text{C}$  showing mixed tetramers **16**, **17**, and **21**. LiHMDS is indicated by an asterisk (\*).

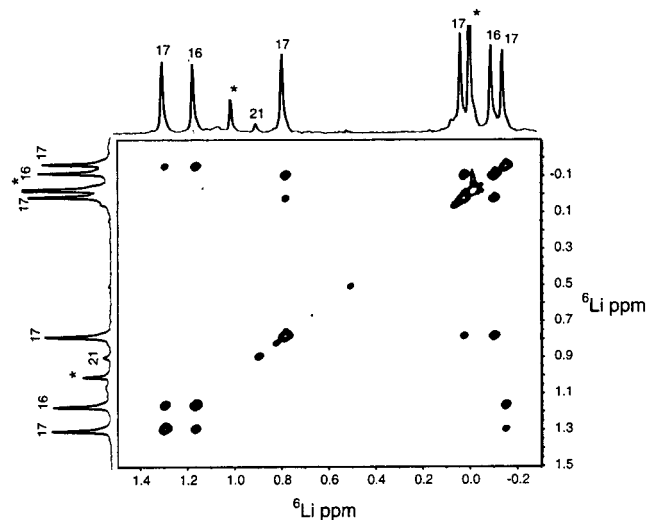


**Figure 5.**  $^6\text{Li},^6\text{Li}$ -exchange (EXSY) spectrum ( $\tau = 1.5\text{ s}$ ) recorded on a 1:1 mixture of  $[\text{}^6\text{Li}]\text{LiCPA}$  (0.5 M) and  $[\text{}^6\text{Li},^{15}\text{N}]\mathbf{10b}$  (0.5 M) in 80% THF/pentane at  $-115\text{ }^\circ\text{C}$  showing mixed tetramers **16**, **17**, and **21**. LiHMDS is indicated by an asterisk (\*).

reveal a mixture of dimer **13** and ladder **14**. Mixed dimer **13**



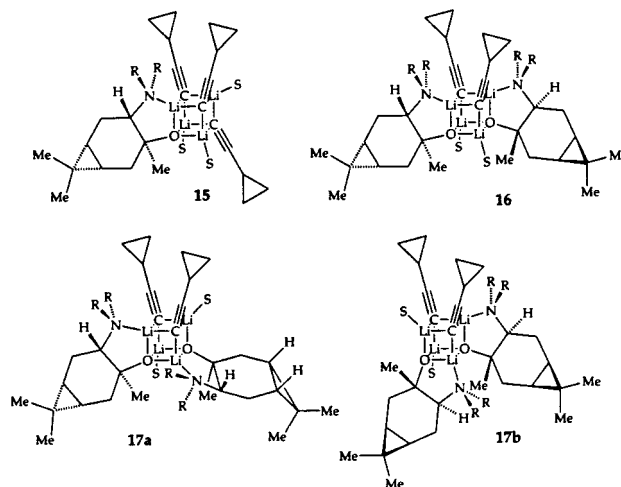
displays a  $^6\text{Li}$  resonance coupled to one LiHMDS subunit and one LiCPA subunit (Table 1). Mixed ladder **14** displays two  $^6\text{Li}$  resonances (2:1) coupled to a pair of LiHMDS subunits. Each  $^6\text{Li}$  is also coupled to the single LiCPA subunit, confirming the ladder motif.  $[\text{}^6\text{Li}]\text{LiHMDS}/[\text{}^6\text{Li}]\mathbf{10b}$  in  $\text{Me}_2\text{NEt}$  and  $[\text{}^6\text{Li}]\text{LiHMDS}/[\text{}^6\text{Li}]\text{LiCPA}$  in  $\text{Et}_2\text{O}$  are heterogeneous.  $^6\text{Li}$  NMR spectra recorded on  $[\text{}^6\text{Li}]\text{LiHMDS}/[\text{}^6\text{Li}]\mathbf{10b}$  in  $\text{Et}_2\text{O}$  display overlapping resonances that were not investigated further.

(31) Leading references to  $\text{RLi}/\text{R}_2\text{NLi}$  mixed aggregates: Balamraju, Y.; Sharp, C. D.; Gammill, W.; Manuel, N.; Pratt, L. M. *Tetrahedron* **1999**, *54*, 7357. Arvidsson, P. I.; Hilmersson, G.; Davidsson, O. *Chem. Eur. J.* **1999**, *5*, 2348.

**Mixed Aggregates in THF/Hydrocarbons.** The requirement that samples be aged to obtain optimum enantioselectivities in the 1,2-additions<sup>6</sup> appears to have a structural component. For example, mixtures of  $[\text{}^6\text{Li}]\text{LiCPA}/[\text{}^6\text{Li}]\mathbf{10b}$  prepared and maintained at  $\leq -78\text{ }^\circ\text{C}$  show primarily the homoaggregates and some unidentified mixed aggregates (Figure 1C). Re-recording the spectra at low temperature after warming the sample to room temperature for 10 min shows conversion to exclusively mixed aggregates (Figure 1E). The spectra remain unchanged after further aging. A more careful analysis reveals that the equilibration becomes appreciable at  $-40\text{ }^\circ\text{C}$ . Extensive aging at  $60\text{ }^\circ\text{C}$ , suggested to be important from the empirical studies,<sup>1,6</sup> caused no detectable changes in aggregate structure. All solutions were aged at room temperature before spectroscopic analysis.

Spectra recorded on  $[\text{}^6\text{Li}]\text{LiCPA}/[\text{}^6\text{Li}]\mathbf{10b}$  mixtures in THF/hydrocarbon solutions revealed a range of mixed aggregates related by a series of balanced equilibria. The initial investigations using THF/pentane mixtures provided confounding results that deviated markedly from those obtained from LiCPA/**8** mixtures reported previously.<sup>10</sup> This confusion was resolved as follows.

$^6\text{Li}$  NMR spectroscopic analysis of a 3:1 mixture of  $[\text{}^6\text{Li}]\text{LiCPA}$  and  $[\text{}^6\text{Li}]\mathbf{10b}$  in 4:1 THF/pentane at  $-115\text{ }^\circ\text{C}$  showed little evidence of 3:1 mixed tetramer **15** that was anticipated



based on previous investigations of LiCPA mixed aggregation.<sup>10</sup> Instead, incremental increases in the proportion of alkoxide **10b** revealed six resonances of approximately equal intensity. (The resonances are correctly labeled as **16** and **17** in Figure 1; see below.) We *incorrectly* postulated the existence of a prismatic hexamer for several reasons: (1) The relative intensities of the six resonances were independent of the LiCPA/**10b** ratio, which is consistent with their being part of the same aggregate (Figure 1D,E). (2) A closely related hexamer of the general form  $(\text{RCCLi})_2(\text{R}^*\text{OLi})_4$  ( $\text{R}^*\text{OLi} = \mathbf{8}$ ) was characterized crystallographically,<sup>11</sup> and a seemingly related  $(\text{RCCLi})_2(\text{RNHLi})_4$  mixed hexamer was characterized spectroscopically.<sup>32</sup> The  $^6\text{Li}$  and  $^{13}\text{C}$  NMR spectroscopic data led us to believe that we were observing a hexamer of the general structure  $(\text{LiCPA})_3(\mathbf{10b})_3$ .  $^{13}\text{C}$  NMR spectra recorded on mixtures of  $[\text{}^6\text{Li},^{13}\text{C}]\text{LiCPA}$  and  $[\text{}^6\text{Li}]\mathbf{10b}$  contain three new  $^{13}\text{C}$  resonances (Figure 3).  $^6\text{Li}$  and  $^{15}\text{N}$  NMR spectra recorded on mixtures of  $[\text{}^6\text{Li}]\text{LiCPA}$  and  $[\text{}^6\text{Li},^{15}\text{N}]\mathbf{10b}$  show  $^6\text{Li}-^{15}\text{N}$  coupling to three  $^6\text{Li}$  nuclei (Figure 4). However, the three  $^{13}\text{C}$  resonances of an asymmetric 3:3 mixed hexamer should each display coupling to three magnetically inequivalent  $^6\text{Li}$  resonances.  $^6\text{Li},^{13}\text{C}$ -HMQC spectra re-

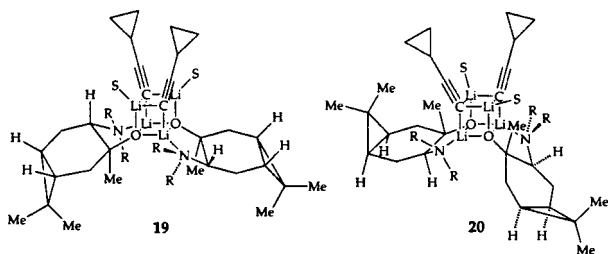
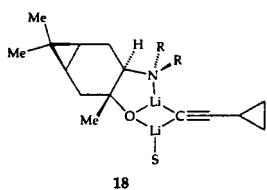
(32) Aubrecht, K. B.; Lucht, B. L.; Collum, D. B. *Organometallics* **1999**, *18*, 2981.

corded on mixtures of  $[^6\text{Li},^{13}\text{C}]\text{LiCPA}$  and  $[^6\text{Li}]\mathbf{10b}$  revealed that one of the three  $^{13}\text{C}$  resonances is split by only two  $^6\text{Li}$  resonances (Figure 3), suggesting that the hexamer attribution was incorrect.

Replacing pentane with toluene as the cosolvent elicited two important structural and spectral changes.<sup>33,34</sup> First, the six resonances that had maintained nearly equal intensities over all LiCPA/**10b** ratios in THF/pentane (Figure 1E) appeared as a relatively high-intensity group of four resonances and a low-intensity pair of resonances (Figure 1F). Second, the missing 3:1 mixed aggregate **15** emerged from what was previously seen as mounds (Figure 1D). By incrementally replacing pentane with toluene, we found that **15** emerged from the mounds as the result of a coalescence rather than by a solvent-dependent change in concentration. The assignments of **15**, **16**, and **17a** or **17b** (denoted as simply **17**) were made as follows.

Of the four resonances attributed to the 3:1 mixed aggregate **15**, three show coupling to two carbons. (See Supporting Information.) One of those three also show  $^6\text{Li}$ - $^{15}\text{N}$  coupling to a coordinated morpholino group of  $[^6\text{Li},^{15}\text{N}]\mathbf{10b}$ . The fourth  $^6\text{Li}$  resonance shows coupling to all three  $^{13}\text{C}$  resonances. The coupling of each  $^{13}\text{C}$  resonance to three  $^6\text{Li}$  resonances confirms that the 3:1 mixed tetramer is a cubic tetramer rather than a four-rung ladder (see Discussion).<sup>35</sup>

$C_2$ -symmetric 2:2 mixed tetramer **16** displays highly characteristic spectroscopic properties. Two  $^6\text{Li}$  resonances in a 1:1 ratio are consistent with a mixed dimer or any of three possible 2:2 mixed tetramers. Spectra recorded on analogous solutions of  $[^6\text{Li},^{13}\text{C}]\text{LiCPA}/[^6\text{Li}]\mathbf{10b}$  display the  $^6\text{Li}$  resonance at  $\delta$  1.16 ppm as a triplet, indicating coupling with two LiCPA subunits (excluding a mixed dimer **18**). The  $^6\text{Li}$  resonance at  $\delta$  -0.11



ppm appears as a doublet, indicating coupling to one LiCPA (Figure 2). The  $^{13}\text{C}$  NMR spectrum displays predominantly a broad multiplet at  $\delta$  114.3 ppm, shown by  $^6\text{Li},^{13}\text{C}$ -HMQC spectroscopy (Figure 3) to be coupled to both  $^6\text{Li}$  resonances.

(33) Pronounced hydrocarbon effects on the rates of anionic polymerizations remain largely unexplained (ref 34).

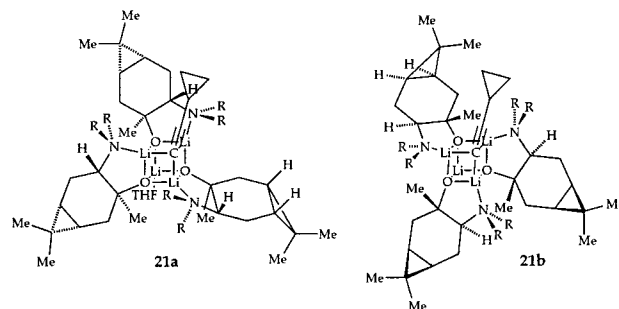
(34) Hsieh, H. L.; Quirk, R. P. *Anionic Polymerization: Principles and Practical Applications*; Marcel Dekker: New York, 1996. Also, see: Lucht, B. L.; Collum, D. B. *J. Am. Chem. Soc.* **1996**, *118*, 2217. Wu, S.; Lee, S.; Beak, P. *J. Am. Chem. Soc.* **1996**, *118*, 715. Ma, J. C.; Dougherty, D. A. *Chem. Rev.* **1997**, *97*, 1303. Chadwick, S. T.; Rennels, R. A.; Rutherford, J. L.; Collum, D. B. *J. Am. Chem. Soc.* **2000**, *122*, 8640. Lewis, H. L.; Brown, T. L. *J. Am. Chem. Soc.* **1970**, *92*, 4664.

(35) Leading reference to organolithium ladders: Gregory, K.; Schleyer, P. v. R.; Snaith, R. *Adv. Inorg. Chem.* **1991**, *37*, 47. Mulvey, R. E. *Chem. Soc. Rev.* **1991**, *20*, 167. Beswick, M. A.; Wright, D. S. In *Comprehensive Organometallic Chemistry II*; Abels, E. W.; Stone, F. G. A., Wilkinson, G., Eds.; Pergamon: New York, 1995; Vol. 1, Chapter 1. Mulvey, R. E. *Chem. Soc. Rev.* **1998**, *27*, 339.

A combination of  $^{15}\text{N}$  NMR spectroscopy and  $^6\text{Li},^{15}\text{N}$ -HMQC spectroscopy (Figure 4) showed  $^{15}\text{N}$  coupling to the  $^6\text{Li}$  resonance also showing coupling to two LiCPA subunits. Among the three  $C_2$ -symmetric 2:2 cubic mixed tetramers (**16**, **19**, and **20**), **16** is the only isomer containing two symmetry-equivalent  $^6\text{Li}$  nuclei concurrently connected to two carbonyl and coordinated by the morpholino nitrogens. Thus, the spectral data establish **16** as the observable  $C_2$ -symmetric 2:2 mixed tetramer. (A comparison with alternative ladder structures is deferred to the Discussion section.)

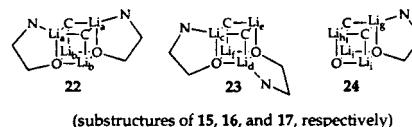
The assignment of the four  $^6\text{Li}$  resonances of equal intensity to a single asymmetric mixed tetramer **17a** or **17b** (denoted as **17** on the spectra) stems directly from the  $^6\text{Li}$ - $^{13}\text{C}$  and  $^6\text{Li}$ - $^{15}\text{N}$  coupling patterns. Two of the  $^6\text{Li}$  resonances are coupled to two LiCPA subunits (LiC<sub>2</sub>O subunits) and the other two  $^6\text{Li}$  resonances are coupled to one adjoining LiCPA subunit (LiCO<sub>2</sub> subunits). Only one LiC<sub>2</sub>O subunit and one LiCO<sub>2</sub> subunit display coupling to  $^{15}\text{N}$  nuclei of the morpholino groups. The coupling of both  $^{13}\text{C}$  resonances to both  $^6\text{Li}$  resonances confirms that the four discrete subunits are part of a single aggregate (**17**), ruling out a structural model based on a 1:1 mixture of  $C_2$ -symmetric tetramers **19** and **20**.

$^6\text{Li}$  spectra recorded on solutions of  $[^6\text{Li}]\text{LiCPA}$  containing excess alkoxide  $[^6\text{Li}]\mathbf{10b}$  display a pair of resonances in a 3:1 ratio characteristic<sup>10</sup> of  $C_3$ -symmetric 1:3 mixed tetramer **21a** or **21b** (denoted as **21** on the spectra). Solutions containing



$[^6\text{Li},^{13}\text{C}]\text{LiCPA}/[^6\text{Li}]\mathbf{10b}$  and  $[^6\text{Li}]\text{LiCPA}/[^6\text{Li},^{15}\text{N}]\mathbf{10b}$  show coupling of the major  $^6\text{Li}$  resonance to the  $^{13}\text{C}$  terminal carbon of the LiCPA subunit and to a single  $^{15}\text{N}$  resonance attributable to the three symmetry-equivalent morpholino groups. Stereoisomeric tetramers **21a** or **21b** were not distinguished.

$^6\text{Li}$ -Li-EXSY provided data on the fluxional chelate rings and, in turn, offered insights into intraaggregate relationships in complete accord with assignments **15**–**17**. Figure 5 illustrates exchanges of the six  $^6\text{Li}$  nuclei corresponding to 2:2 mixed tetramers **16** and **17** (labeled Li<sub>a</sub>–Li<sub>f</sub> in partial structures **22** and **23**) and the four  $^6\text{Li}$  nuclei of 3:1 mixed tetramer **15** (labeled



Li<sub>a</sub>–Li<sub>f</sub> in partial structure **24**). Most important, the cross-peaks were detected only for those Li–Li exchanges that can occur by simple movements of the chelate rings. The exchanging pairs include the following: Li<sub>a</sub>–Li<sub>c</sub>; Li<sub>a</sub>–Li<sub>e</sub>; Li<sub>b</sub>–Li<sub>d</sub>; Li<sub>b</sub>–Li<sub>f</sub>; Li<sub>c</sub>–Li<sub>e</sub>; Li<sub>d</sub>–Li<sub>f</sub>; Li<sub>g</sub>–Li<sub>i</sub>; Li<sub>g</sub>–Li<sub>j</sub>; and Li<sub>i</sub>–Li<sub>j</sub>.

**Mixed Aggregates in Me<sub>2</sub>NEt and Et<sub>2</sub>O.** Investigations using poorly coordinating solvents Et<sub>2</sub>O and Me<sub>2</sub>NEt<sup>27,28</sup> (Supporting Information) reveal notable solvent effects. Although the mixed aggregates in THF solutions equilibrate within

10 min at 0 °C, equilibrations in Et<sub>2</sub>O and Me<sub>2</sub>NEt require >4 h at 25 °C. Because Et<sub>2</sub>O and Me<sub>2</sub>NEt are inferior to THF as ligands for lithium,<sup>28</sup> these slower equilibrations suggest a mechanism requiring solvent association. Additionally, THF, Me<sub>2</sub>NEt, and Et<sub>2</sub>O all provide 3:1, 2:2, and 1:3 mixed aggregates. However, the stereochemistry of the 2:2 mixed aggregates is highly solvent-dependent. Me<sub>2</sub>NEt yields asymmetric tetramer **17** as the sole observable 2:2 mixed tetramer, Et<sub>2</sub>O affords only C<sub>2</sub>-symmetric mixed tetramer **16**, and THF provides both stereoisomers.

## Discussion

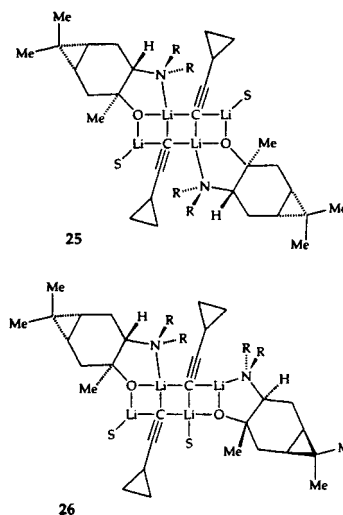
**Summary.** As part of our efforts to understand the highly enantioselective addition to quinazolinones illustrated in eq 2, we initiated studies of the underlying organolithium mixed aggregates. The spectroscopic investigations of the mixed aggregates in LiCPA/**10b** mixtures show significant structural parallels with mixed aggregates in LiCPA/**8** mixtures.<sup>10</sup> In both cases we observed pronounced aging effects: LiCPA/**10b** mixtures required warming to room temperature to equilibrate the resulting mixed aggregates. These aging effects appear to have a measurable impact on the stereochemistry of 1,2-additions.<sup>6,10</sup> In a field dominated by aggregate–aggregate exchanges that are fast on NMR time scales at room temperature, the slow aggregate exchanges on laboratory time scales are exceptional.<sup>18</sup>

At high LiCPA/**10b** ratios, (RCCLi)<sub>3</sub>(R\*OLi) mixed tetramer **15** is formed. At low LiCPA/**10b** ratios, a single C<sub>3</sub>-symmetric (RCCLi)(R\*OLi)<sub>3</sub> mixed tetramer **21a** or **21b** (denoted simply as **21**) predominates. (Tetramers **21a** and **21b** could not be distinguished spectroscopically.) Similar behaviors were noted for LiCPA/**8** mixtures. In contrast, however, the structures observed in equimolar LiCPA/**10b** and LiCPA/**8** mixtures are markedly different. Whereas equimolar LiCPA/**8** mixtures provide a C<sub>2</sub>-symmetric tetramer (analogous to **16**) as the only observable 2:2 mixed tetramer, LiCPA/**10b** mixtures afford an equilibrium of C<sub>2</sub>-symmetric (RCCLi)<sub>2</sub>(R\*OLi)<sub>2</sub> mixed tetramer **16** and a single asymmetric isomer **17a** or **17b** (denoted simply as **17**).

We derived several insights into the stereocontrol of aggregation from investigations of solvent effects. The stereochemistry of the 2:2 mixed aggregate is solvent dependent: THF provides a nearly equimolar mixture of C<sub>2</sub>-symmetric tetramer **16** and asymmetric tetramer **17** (**17a** or **17b**), Et<sub>2</sub>O affords only **16**, and Me<sub>2</sub>NEt affords only **17**. The odd aspect of this trend is that, with respect to their propensities to coordinate to lithium in a hindered environment, the solvents follow the order THF > Et<sub>2</sub>O > Me<sub>2</sub>NEt, largely due to increasing steric demand.<sup>27</sup> It is unclear, therefore, why THF would display intermediate behavior with respect to controlling the stereochemistry of aggregation.

**On the Role of LiHMDS.** In the enantioselective addition shown in eq 2, LiHMDS is uniquely effective at promoting full conversion, optimizing the stereochemistry, and increasing the overall reproducibility of the reaction. Spectroscopic investigations showed that LiHMDS quantitatively lithiates both cyclopropylacetylene and amino caranol **10a**, in turn ensuring that the intended LiCPA/**10b** ratios are maintained. Previous studies had shown that residual amino alcohols are strong ligands for lithium<sup>10</sup> and could be problematic. Moreover, in contrast with the lithium dialkylamides that are highly prone to form mixed aggregates, LiHMDS does not form mixed aggregates with either the LiCPA or alkoxide **10b** in THF. In short, LiHMDS in THF appears to be an ideal proton sponge.

**Ladders vs Cubic Tetramers.** The evidence that the mixed aggregates are cubes rather than four-rung ladders is compelling in most instances. The assignment of the 3:1 mixed tetramer **15**, for example, stems from the Li–C connectivities available from the <sup>6</sup>Li–<sup>13</sup>C couplings. Similarly, the C<sub>3</sub>-symmetry requires that the 1:3 mixed tetramer assigned as **21** is indeed cubic rather than a less symmetric four-rung ladder.<sup>35</sup> The spectroscopic opacity of the Li–O linkages, however, causes the 2:2 mixed tetramers **16** and **17** to be indistinguishable from four-rung ladders **25** and **26**, respectively. Crystallographic studies provide



support to both the cubic and the ladder structural motifs.<sup>26,35,36</sup> The solvent dependence on the pair of 2:2 mixed tetramers could be construed as evidence of two fundamentally different structures, although it is unclear how a ladder-cubic tetramer equilibrium would be influenced by solvent. Overall, we find the analogy with the 1:3 and 3:1 cubic tetramers to be strong, although not unassailable, evidence that the 2:2 mixed tetramers are cubic as well.

**Structure–Reactivity Relationships—The Unknowns.** The spectroscopic studies described herein represent a necessary first step toward understanding the asymmetric additions to the quinazolinones (eq 2). It is important, however, to underscore what is *not* shown by these results. First, we can begin to consider the origins of the enantioselectivities only after we ascertain how lithiated substrate **11** and lithiated product **12** influence aggregate structures. Indeed, ongoing investigations of the additional combinations of LiCPA, **10b**, **11**, **12**, and LiHMDS reveal that **11** and **12** readily form mixed aggregates with both LiCPA and amino alkoxide **10b**. We believe that determining how the different subunits partition among the mixed aggregates will be particularly revealing. Second, we have described LiHMDS as a proton scavenger that avoids participating in potentially complicating mixed aggregation. It is less clear, however, whether (Me<sub>3</sub>Si)<sub>2</sub>NH is inconsequential to the 1,2-addition.

## Experimental Section

**Reagents and Solvents.** THF, Et<sub>2</sub>O, Me<sub>2</sub>NEt, and all hydrocarbons used for the spectroscopic studies were vacuum-transferred from degassed blue or purple stills containing sodium benzophenone ketyl.

(36) For related crystal structures of (*n*-BuLi)(R\*OLi)<sub>3</sub> and (*n*-BuLi)<sub>2</sub>(R\*OLi)<sub>2</sub> mixed aggregates, see: Goldfuss, B.; Khan, S. I.; Houk, K. N. *Organometallics* **1999**, *18*, 2927. Goldfuss, B.; Steigelmann, M.; Rominger, F. *Angew. Chem., Int. Ed. Engl.* **2000**, *39*, 4133. Donkersvoort, J. G.; Vicario, J. L.; Rijnberg, E.; Jastrzebski, J. T. B. H.; Kooijman, H.; Spek, A. L.; van Koten, G. J. *Organomet. Chem.* **1998**, *550*, 463.



The hydrocarbon stills contained 1% tetraglyme to dissolve the ketyl. Air- and moisture-sensitive materials were manipulated using vacuum line and syringe techniques. Amino alcohols **10a** and [<sup>15</sup>N]**10a** were prepared by a literature procedure.<sup>13</sup> [<sup>6</sup>Li]LiCPA and [<sup>6</sup>Li,<sup>13</sup>C]LiCPA were prepared by lithiation of cyclopropylacetylene<sup>37</sup> and [<sup>13</sup>C-2]-cyclopropylacetylene<sup>10</sup> using [<sup>6</sup>Li]*n*-BuLi (unrecrystallized)<sup>38</sup> and isolated as a white solid as described previously.<sup>10</sup> Lithium alkoxide **10b** was generated in situ from **10a** and LiHMDS. [<sup>6</sup>Li]LiHMDS and [<sup>6</sup>Li,<sup>15</sup>N]LiHMDS were isolated as crystalline solids.<sup>16</sup>

**NMR Spectroscopic Analyses.** All NMR tubes were prepared using stock solutions and sealed under vacuum. [<sup>6</sup>Li]LiHMDS and [<sup>6</sup>Li,<sup>15</sup>N]-LiHMDS were kept in slight excess at all times to scavenge the cyclopropylacetylene and amino alcohol **10a**. All NMR tubes were prepared using stock solutions and sealed under vacuum. Standard <sup>6</sup>Li, <sup>15</sup>N, and <sup>13</sup>C NMR spectra were recorded on a Varian XL-400 spectrometer operating at 58.84, 40.52, and 100.58 MHz (respectively) or on a Varian Unity 500 spectrometer operating at 73.57, 58.84, and 125.76 MHz (respectively).<sup>39</sup> The <sup>6</sup>Li, <sup>15</sup>N, and <sup>13</sup>C resonances are referenced to 0.3 M [<sup>6</sup>Li]LiCl/MeOH at -100 °C (0.0 ppm), neat Me<sub>2</sub>NEt at -100 °C (25.7 ppm), and the toluene methyl resonance at -100 °C (20.4 ppm), respectively. The <sup>6</sup>Li-<sup>15</sup>N HMQC spectra were recorded on the Varian Unity 500 spectrometer equipped with a 3-channel probe designed to accommodate lithium and nitrogen pulses custom-built by Nalorac (www.nalorac.com). <sup>6</sup>Li-<sup>6</sup>Li-EXSY,<sup>23</sup> <sup>6</sup>Li,<sup>13</sup>C-HMQC spectroscopy,<sup>20</sup> and <sup>6</sup>Li,<sup>15</sup>N-HMQC spectroscopy<sup>22</sup> are well-established methods. The <sup>1</sup>J(<sup>6</sup>Li,<sup>13</sup>C)-resolved spectroscopy has also been reported, but is relatively untested.<sup>19a</sup> The <sup>1</sup>J(<sup>6</sup>Li,<sup>13</sup>C)-resolved spectra were recorded using existing protocols with some modification.<sup>19b</sup> The <sup>6</sup>Li is observed, and the <sup>13</sup>C pulses used a separate Rf-channel. The first decoupling<sup>19b</sup> was replaced by a 180° pulse on <sup>6</sup>Li. The phases of the two 180° pulses are the same. Due to this specific implementation,

(37) [2-<sup>13</sup>C]Cyclopropylacetylene used to prepare lithium acetylide [2-<sup>13</sup>C]**4** was synthesized from cyclopropane carboxaldehyde and [<sup>13</sup>C]CBr<sub>4</sub> by a literature procedure: Baldwin, J. E.; Villarica, K. A. *J. Org. Chem.* **1995**, *60*, 186. Also, see ref 7.

(38) Kottke, T.; Stalke, D. *Angew. Chem., Int. Ed. Engl.* **1993**, *32*, 580. Rennels, R. A.; Maliakal, A.; Collum, D. B. *J. Am. Chem. Soc.* **1998**, *120*, 421.

(39) Hall, P.; Gilchrist, J. H.; Harrison, A. T.; Fuller, D. J.; Collum, D. B. *J. Am. Chem. Soc.* **1991**, *113*, 9575.

the splittings in the <sup>1</sup>J(<sup>6</sup>Li,<sup>13</sup>C)-resolved spectra are identical to those in the standard <sup>6</sup>Li spectra instead of 1/2J as described. The pulse sequence for the <sup>6</sup>Li,<sup>6</sup>Li-EXSY was implemented in states mode to obtain pure absorption spectra. To determine the exchange rates quantitatively, exchange spectra were taken at several different mixing times (τ<sub>m</sub>) ranging from 0.5 to 4.0 s, consecutively. The EXSY cross-peak volumes were measured as the intensity by using the NMRPipe software. For a short τ<sub>m</sub> the dependence of the intensity (I<sub>ij</sub>) of the EXSY cross-peak between species *i* and *j* on the mixing time is

$$I_{ij} = ak_{ij}C_j\tau_m - (1/2)b_{ij}C_j\tau_m^2$$

where *k*<sub>ij</sub> is the forward exchange rate from *i* to *j*, *C*<sub>*j*</sub> is the concentration of *j*, *a* is a constant for converting the concentration *C*<sub>*j*</sub> to the magnetization of *j*, and *b*<sub>ij</sub> is a constant for secondary exchanges. The build-up curves were constructed by the least-squares fitting of the experimental data with a secondary polynomial function. The first-order coefficient (*a*<sub>ij</sub>) of the fitting is then proportional to the product *k*<sub>ij</sub>*C*<sub>*j*</sub>:

$$a_{ij} \propto k_{ij}C_j = k_{ji}C_i$$

where the equality between *k*<sub>ij</sub>*C*<sub>*j*</sub> and *k*<sub>ji</sub>*C*<sub>*i*</sub> is the equilibrium between *i* and *j*.

**Acknowledgment.** The Cornell group thanks the National Institutes of Health and DuPont Pharmaceuticals for direct support of this work. We also thank DuPont, Merck, Pfizer, and Boehringer-Ingelheim for indirect support. We acknowledge the National Science Foundation Instrumentation Program (CHE 7904825 and PCM 8018643), the National Institutes of Health (RR02002), and IBM for support of the Cornell Nuclear Magnetic Resonance Facility.

**Supporting Information Available:** NMR spectra (PDF). This material is available free of charge via the Internet at <http://pubs.acs.org>.

JA0105616